Research article JHEP|Reports

CD14 facilitates perinatal human cytomegalovirus infection in biliary epithelial cells via CD55

Authors

Liang Su, Yan Chen, Ming Fu, Hezhen Wang, Yanlu Tong, Zefeng Lin, Hongjiao Chen, Huiting Lin, Yi Chen, Bing Zhu, Sige Ma, Yiyi Xiao, Junyu Huang, Ziyang Zhao, Fenjie Li, Rongchen Ye, Hongguang Shi, Zhe Wang, Jixiao Zeng, Zhe Wen, Minhua Luo, Huimin Xia, Ruizhong Zhang

Correspondence

xia-huimin@foxmail.com (H. Xia), zhangruizhong@gwcmc.org (R. Zhang).

Graphical abstract

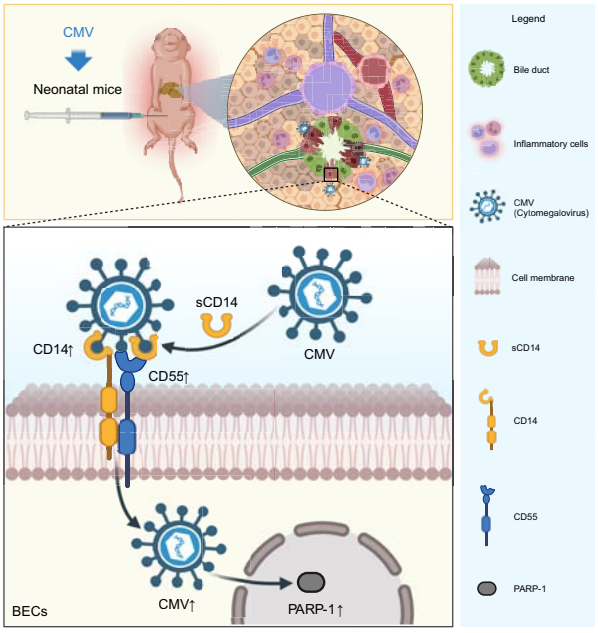

Highlights

- CD14 facilitates perinatal HCMV infection in biliary epithelial cells (BECs) via CD55.
- PARP-1-mediated cell death was detected in perinatal CMV-infected BECs.
- CD14 knockout delays the onset of illness and reduces MCMV-induced bile duct damage in mice.
- Administration of anti-mouse CD14 antibody and PARP-1 inhibitor treatment in MCMV-infected mice resulted in amelioration of bile duct damage and reduced mortality.

Impact and implications

Perinatal human cytomegalovirus (HCMV) infection is associated with bile duct damage, but the underlying mechanism is still unknown. We discovered that CD14 expression is increased in biliary epithelial cells during perinatal HCMV infection and facilitates viral entry through CD55. We also detected PARP-1-mediated cell death in perinatal HCMV-infected biliary epithelial cells. We showed that blocking CD14 or inhibiting PARP-1 reduced bile duct damage and mortality in a mouse model of murine cytomegalovirus infection. Our findings provide a new insight into therapeutic strategies for perinatal HCMV infection.

https://doi.org/10.1016/j.jhepr.2024.101018

Research article

JHEP|Reports

CD14 facilitates perinatal human cytomegalovirus infection in biliary epithelial cells via CD55

Liang Su,[1,2,†] **Yan Chen**,[1,3,†] **Ming Fu**,[1,4,†] Hezhen Wang,[1] Yanlu Tong,[1] Zefeng Lin,[1] Hongjiao Chen,[1] Huiting Lin,[1] Yi Chen,[1] Bing Zhu,[1] Sige Ma,[1] Yiyi Xiao,[1] Junyu Huang,[1] Ziyang Zhao,[1] Fenjie Li,[1] Rongchen Ye,[1] Hongguang Shi,[5] Zhe Wang,[1] Jixiao Zeng,[1] Zhe Wen,[1] Minhua Luo,[3] Huimin Xia,[1,*] Ruizhong Zhang[1,5,*]

[1]*Provincial Key Laboratory of Research in Structure Birth Defect Disease and Department of Pediatric Surgery, Guangdong Provincial Clinical Research Center for Child Health, Guangzhou Women and Children's Medical Center, Guangzhou Medical University, Guangzhou, China;* [2]*Key Laboratory of Special Pathogens and Biosafety, Wuhan Institute of Virology, Chinese Academy of Sciences, Wuhan, China;* [3]*Faculty of Medicine, Macau University of Science and Technology, Macau SAR, China;* [4]*Institute Pasteur of Shanghai, Chinese Academy of Sciences, Shanghai, China;* [5]*Department of Pediatric Surgery, The Third Affiliated Hospital of Zhengzhou University, Zhengzhou, China*

JHEP Reports **2024.** https://doi.org/10.1016/j.jhepr.2024.101018

Background & Aims: A high human cytomegalovirus (HCMV) infection rate accompanied by an increased level of bile duct damage is observed in the perinatal period. The possible mechanism was investigated.

Methods: A total of 1,120 HCMV-positive and 9,297 HCMV-negative children were recruited, and depending on age, their liver biochemistry profile was compared. Fetal and infant biliary epithelial cells (F-BECs and I-BECs, respectively) were infected with HCMV, and the differences in cells were revealed by proteomic analysis. Protein–protein interactions were examined by coimmunoprecipitation and mass spectrometry analyses. A murine cytomegalovirus (MCMV) infection model was established to assess treatment effects.

Results: Perinatal HCMV infection significantly increased the level of bile duct damage. Neonatal BALB/c mice inoculated with MCMV showed obvious inflammation in the portal area with an abnormal bile duct structure. Proteomics analysis showed higher CD14 expression in F-BECs than in I-BECs. CD14 siRNA administration hindered HCMV infection, and CD14-knockout mice showed lower MCMV-induced bile duct damage. HCMV infection upregulated CD55 and poly ADP-ribose polymerase-1 (PARP-1) expression in F-BECs. Coimmunoprecipitation and mass spectrometry analyses revealed formation of the CD14–CD55 complex. siRNA-mediated inhibition of CD55 expression reduced sCD14-promoted HCMV replication in F-BECs. In MCMV-infected mice, anti-mouse CD14 antibody and PARP-1 inhibitor treatment diminished cell death, ameliorated bile duct damage, and reduced mortality.

Conclusions: CD14 facilitates perinatal HCMV infection in BECs via CD55, and PARP-1-mediated cell death was detected in perinatal cytomegalovirus-infected BECs. These results provide new insight into the treatment of perinatal HCMV infection with bile duct damage.

Impact and implications: Perinatal human cytomegalovirus (HCMV) infection is associated with bile duct damage, but the underlying mechanism is still unknown. We discovered that CD14 expression is increased in biliary epithelial cells during perinatal HCMV infection and facilitates viral entry through CD55. We also detected PARP-1-mediated cell death in perinatal HCMV-infected biliary epithelial cells. We showed that blocking CD14 or inhibiting PARP-1 reduced bile duct damage and mortality in a mouse model of murine cytomegalovirus infection. Our findings provide a new insight into therapeutic strategies for perinatal HCMV infection.

Introduction

The global rate of human cytomegalovirus (HCMV) infection is approximately 83%,[1] with approximately 80% of infections occurring in children younger than 5 years in China.[2] Depending on the infection timeline, HCMV infection can be classified as congenital infection, postnatal infection before 2 weeks, perinatal infection (3–12 weeks postnatally), and acquired infection (>12 weeks postnatally).[3] Among the three age groups, the proportion of congenital infection is relatively low, affecting approximately 0.2–2.2% of neonates,[4] and acquired infection generally presents as latent infection, wherein patients have no

Keywords: Cytomegalovirus; Perinatal period; CD14; CD55; Biliary epithelial cells; PARP-1.

Received 10 June 2023; received in revised form 28 November 2023; accepted 8 January 2024; available online 26 January 2024

† These authors are designated as co-first authors.

* Corresponding authors. Addresses: Provincial Key Laboratory of Research in Structure Birth Defect Disease, Guangdong Provincial Clinical Research Center for Child Health, Guangzhou Women and Children's Medical Center, Guangzhou Medical University, No. 9, Jinshui Road, Guangzhou, 510623, Guangdong, China. Tel.: +86-20-3807 6560; Fax. +86-20-3807-6020.

E-mail addresses: xia-huimin@foxmail.com (H. Xia), zhangruizhong@gwcmc.org (R. Zhang).

obvious symptoms. The infection rate of perinatal HCMV is much higher than that of congenital HCMV, ranging from 10 to 15%.[5] Liver damage, such as cholestatic hepatitis, is one of the important pathological changes that occurs with perinatal HCMV infection. With inappropriate treatment, the disease can further progress, leading to serious complications, such as portal hypertension, cirrhosis, and liver failure.[6] However, the detailed mechanism of bile duct injury caused by HCMV is still not clear.

The perinatal period is a critical period in the development of the biliary tract. At birth, the biliary tract system has not been fully developed, and most biliary epithelial cells (BECs) are still in the immature stage and need to gradually develop into bile ducts with tubular structures. Therefore, these cells are extremely vulnerable to damage caused by infectious pathogenic factors.[7] Perinatal HCMV infection was reported to cause inflammatory lesions of BECs and result in poor bile outflow, intrahepatic and extrahepatic cholestasis, and severe fibrosis, stenosis, or atresia of the bile duct.[3,8] Further analysis of HCMV infection in BECs is needed.

In this study, we retrospectively analyzed the clinical and biochemical characteristics of HCMV-positive individuals. Three molecules, namely CD14, CD55, and poly ADP-ribose polymerase-1 (PARP-1), were identified by proteomic profiling analysis and gene/protein interference techniques in an HCMV-infected BEC culture system *in vitro*. The application of CD14-neutralizing antibodies, PARP-1 inhibitor, and $CD14^{-/-}$ C57BL/6 mice revealed the importance of these molecules in the development of bile duct damage in an MCMV-infected newborn mouse model. This study elucidates the mechanism responsible for the perinatal HCMV susceptibility of BECs and partially explains the phenomenon of bile duct injury in the perinatal period.

Patients and methods

Clinical study

The participants in HCMV-negative group (HCMV−, n = 9,297) and those in the HCMV-positive group (HCMV+, n = 1,120) were recruited at Guangzhou Women and Children's Medical Center (Guangzhou, China). Fresh peripheral blood samples from HCMV+ and HCMV− children were obtained and used for HCMV detection and liver biochemistry. The diagnostic criteria for HCMV positivity were HCMV DNA amplification in plasma/cerebrospinal fluid/urine/sputum/bronchoalveolar lavage fluid/throat swabs/ascites (quantitative PCR [qPCR] quantification of HCMV DNA >500 copies/ml) or HCMV IgM positivity in plasma.

Mice, viruses, and cells

Prenatal BALB/c mice (aged 10–12 weeks and weighing 35–40 g) were purchased from Guangdong Provincial Animal Laboratory Center (Guangzhou, China). $CD14^{-/-}$ C57BL/6 mice were prepared and certified by Cyagen Biotech, Inc. (CA, USA). All animal experiments were carried out at the Experimental Animal Center of Guangzhou Medical University (Guangzhou, China). The MCMV K181 strain and HCMV Towne strain were obtained from the State Key Laboratory of Virology, Wuhan University, China. MCMV was amplified in mouse embryonic fibroblasts (National Institutes of Health 3T3), HCMV was amplified in human foreskin fibroblasts, and the viral titer was determined by plaque-forming unit assay. Human fetal biliary epithelial cells (F-BECs) isolated from organ donors (23 weeks of gestation, female) were provided by ScienCell Research Laboratories (CA, USA), and human infant biliary epithelial cells (I-BECs) isolated from organ donors (6 months, male) were provided by ZenBio Company (NC, USA). The details of the MCMV-infected mouse model and treatment, HCMV–BEC coculture and CD14/CD55 RNA interference, and related immunohistological, functional, and molecular detections and statistical analysis are described in the Supplementary Materials and Methods.

Study approval

The clinical study was approved by the Clinical Research Institutional Review Committee of Guangzhou Women and Children's Medical Center (Approval No. 34500). Written informed consent was obtained from all the participants before the study. The animal experiment program was approved by the Animal Protection and Use Committee of the Experimental Animal Center of Guangzhou Medical University (Ethics Code: IACUC-DB-16-0602).

Results

Perinatal HCMV infection is accompanied by bile duct injury

To evaluate the incidence of HCMV infection in children, we analyzed 1,120 HCMV+ children and 9,297 HCMV− children (Fig. 1A). In a comparison of congenital infection (≤2 weeks) and acquired infection (>12 weeks), the number of cases during the perinatal period (3–12 weeks postnatally) was the highest, and the proportion was 61.52% in all HCMV+ patients analyzed (Fig. 1B and C). For the clinical characteristics, liver biochemistry was assessed. Perinatal HCMV infection significantly increased the levels of bile duct damage-related molecules, such as γ-glutamyl transpeptidase (γ-GT), direct bilirubin (DBIL), and total bile acid (TBA) (Fig. 1D), and hepatocyte damage-related molecules, such as alanine aminotransferase (ALT) and aspartate aminotransferase (AST) (Fig. S1A), suggesting developmental stage-related HCMV infection in the perinatal period and the possibility of bile duct damage induced by viral infection.

To further investigate the time-dependent hepatobiliary damage caused by cytomegalovirus (CMV) infection, based on the results of an RNA sequencing analysis, which showed that the mRNA expression of the BEC maturation-related markers epithelial cell adhesion molecule (EpCAM), cytokeratin 19 (CK19), and Sox9 in BALB/c mice on Day 6 after birth was significantly higher than that on Day 1 after birth (Fig. S1B), BALB/c mice were inoculated with MCMV on Day 1 or Day 10 after birth to simulate HCMV infection at different maturation stages of BECs (Fig. S1C). The results showed that compared with the group infected with virus on Day 10 after birth, growth delay, reduced body weight, reduced survival rate, and obvious inflammatory necrotic spots on the surface of the liver were observed in the early infection group (Fig. 1E and F, and Fig. S1D and E). The clinical laboratory examination results showed upregulated expression of bile duct and hepatocyte damage-related molecules such as γ-GT, DBIL, TBA, alkaline phosphatase (ALP), total bilirubin (TBIL), indirect bilirubin (IBIL), ALT, and AST (Fig. 1G and Fig. S1F). In addition, MCMV immediate early protein IE1 gene expression in BECs in the early virus infection group was significantly increased compared with that in the group infected on Day 10 after birth (Fig. 1H). Furthermore, flow

cytometry analysis showed significantly increased total cell death (Annexin-V$^+$, 7-AAD$^+$, and double$^+$) level of EpCAM$^+$ BECs in the liver (Fig. S3A and Fig. 1I). The liver sections showed infiltration of immune cells in the portal area and disordered intrahepatic bile duct numbers, which were significantly increased (Fig. S1G and H).

HCMV infection in F-BECs causes cell death

To demonstrate the effect of HCMV infection on perinatal BECs, F-BECs were further examined and compared with I-BECs by coculture with HCMV *in vitro*. Immunofluorescence staining showed that the protein expression of the BEC progenitor marker AFP in F-BECs was significantly higher than that in I-BECs, and the protein expression of the BEC maturation marker CK19 in F-BECs was significantly lower than that in I-BECs (Fig. S2A). The coculture results indicated that the proliferation of F-BECs after HCMV infection was reduced, and the cells were swollen and detached from the culture plate, whereas I-BECs with HCMV infection had growth comparable with that of the control group without virus (Fig. 2A). Furthermore, flow cytometric analysis showed significantly increased total cell death level of F-BECs after HCMV infection (Fig. 2B and C). Meanwhile, the relative viral load determined by qPCR in cell culture supernatants was significantly increased in F-BECs (Fig. 2D). The mRNA and protein expression of the intracellular viral structure protein pp65 and the levels of the immediate early protein IE1 were significantly increased in F-BECs compared with I-BECs, as determined by qPCR and immunofluorescence (Fig. 2E and F). These results indicated that active infection with HCMV preferentially occurs in F-BECs and results in increased cell death compared with that in I-BECs.

CD14 produced by F-BECs promotes HCMV infection

To further analyze the susceptibility of F-BECs to HCMV infection, the protein expression in F-BECs and I-BECs on Day 3 was determined and compared by tandem mass tag labeling-based quantitative proteomics. The results showed that 42 proteins showed upregulated expression, and 11 proteins showed downregulated expression in F-BECs compared with I-BECs (Fig. 3A and Fig. S2B). The proteins with upregulated expression were analyzed using Metascape. The results showed that most proteins were related to cell development and differentiation (Fig. 3B). Gene ontology (GO) DisGeNET analysis showed that some of these proteins were related to liver diseases, such as congenital atresia of the extrahepatic bile duct, biliary atresia, and liver fibrosis (Fig. 3C). The significantly increased proteins in F-BECs included CD14, ICAM1, and CTNNB1, and the related expression of the proteins in I-BECs and F-BECs is shown in Fig. S2B and C. In particular, HCMV infection in CD14$^+$ monocytes had been well established as a cellular model, and the expression of CD14 was found to be increased significantly in F-BECs. Whether this protein plays a role in HCMV infection of cells is unknown. qPCR and immunofluorescence results showed that the CD14 mRNA and protein levels were significantly increased in F-BECs compared with I-BECs (Fig. 3D and E), suggesting the potential role of CD14 in CMV infection in F-BECs. Two forms of CD14 were found in BECs: a transmembrane protein (mCD14) and a soluble protein (sCD14). The mCD14 and sCD14 expression levels in F-BECs were both higher than those in the I-BECs with or without virus infection (Fig. 3F and G), indicating that CD14 may play an important role in viral infection in F-BECs. After administration of siRNA targeting CD14 in F-BECs, reductions in the CD14 mRNA and protein levels and mCD14 and sCD14 protein levels were observed (Fig. S2D–G). qPCR and immunofluorescence results showed that the mRNA and protein levels of pp65 and the protein level of IE1 in the CD14 siRNA group were significantly decreased compared with those in the control group (Fig. 3H and I), suggesting that F-BECs may be prone to HCMV infection caused by the production of CD14.

MCMV infection causes bile duct damage in mice via CD14

To further confirm the essential role of CD14 in HCMV infection of BECs, flow cytometry analysis showed that CD14 protein expression on EpCAM$^+$ BECs in the livers of mice on Day 1 after birth was significantly higher than that on Day 10 after birth (Fig. S3A and B). Compared with MCMV-infected wild-type (WT) C57BL/6 mice, CD14$^{-/-}$ C57BL/6 mice were infected with MCMV on the first day after birth. The results showed that when compared with that of nontreated WT mice, the growth of MCMV-infected WT mice was significantly impaired (Fig. 4A), with reduced body weight (Fig. S3C) and the levels of liver inflammation and hepatocyte injury-related indicators significantly increased (Fig. 4B and C, and Fig. S3E). However, when compared with the WT + MCMV group, the MCMV-infected CD14$^{-/-}$ mice had normal growth (Fig. 4A), no significant difference in body weight or survival rate (Fig. S3C and D), and no liver inflammation or necrotic lesions (Fig. 4B). The indexes related to bile duct and hepatocyte injury were significantly reduced (Fig. 4C and Fig. S3E). The number of infiltrating immune cells in the portal area and disordered intrahepatic bile ducts were significantly reduced (Fig. S3F and G). MCMV immediate early protein IE1 gene expression in BECs was significantly decreased (Fig. 4D), and flow cytometry analysis showed significantly decreased total cell death level of EpCAM$^+$ BECs in the liver (Fig. 4E). These results indicated that CD14 deficiency prevents MCMV infection and reduces BEC damage.

CD14 partially promotes HCMV entry into cells via CD55 receptors

To further analyze the protein profile changes after HCMV infection of BECs, tandem mass tag labeling-based quantitative proteomics was used to determine the difference in the protein expression of F-BECs before and after HCMV infection on Day 4. The results showed that after HCMV infection, 122 proteins showed upregulated expression, and 134 proteins showed downregulated expression (Fig. 5A). The proteins with upregulated expression were further analyzed using Metascape. The results showed that most pathways were related to protein modifications, such as protein folding and cellular amino acid metabolic processes. The necroptosis pathway partially explained the cell death after HCMV infection (Fig. 5B). Then, GO DisGeNET analysis showed that the virus infection pathways were enhanced (Fig. 5C). SAA2, a major acute-phase reactant, had the greatest changes in $\log_2$(fc) when compared with the control, and CD55 expression was strongly increased after HCMV infection in F-BECs (Fig. 5A and Fig. S4A). The expression of CD55 was further confirmed by qPCR and immunofluorescence and found to be significantly increased (Fig. 5D and E). Flow

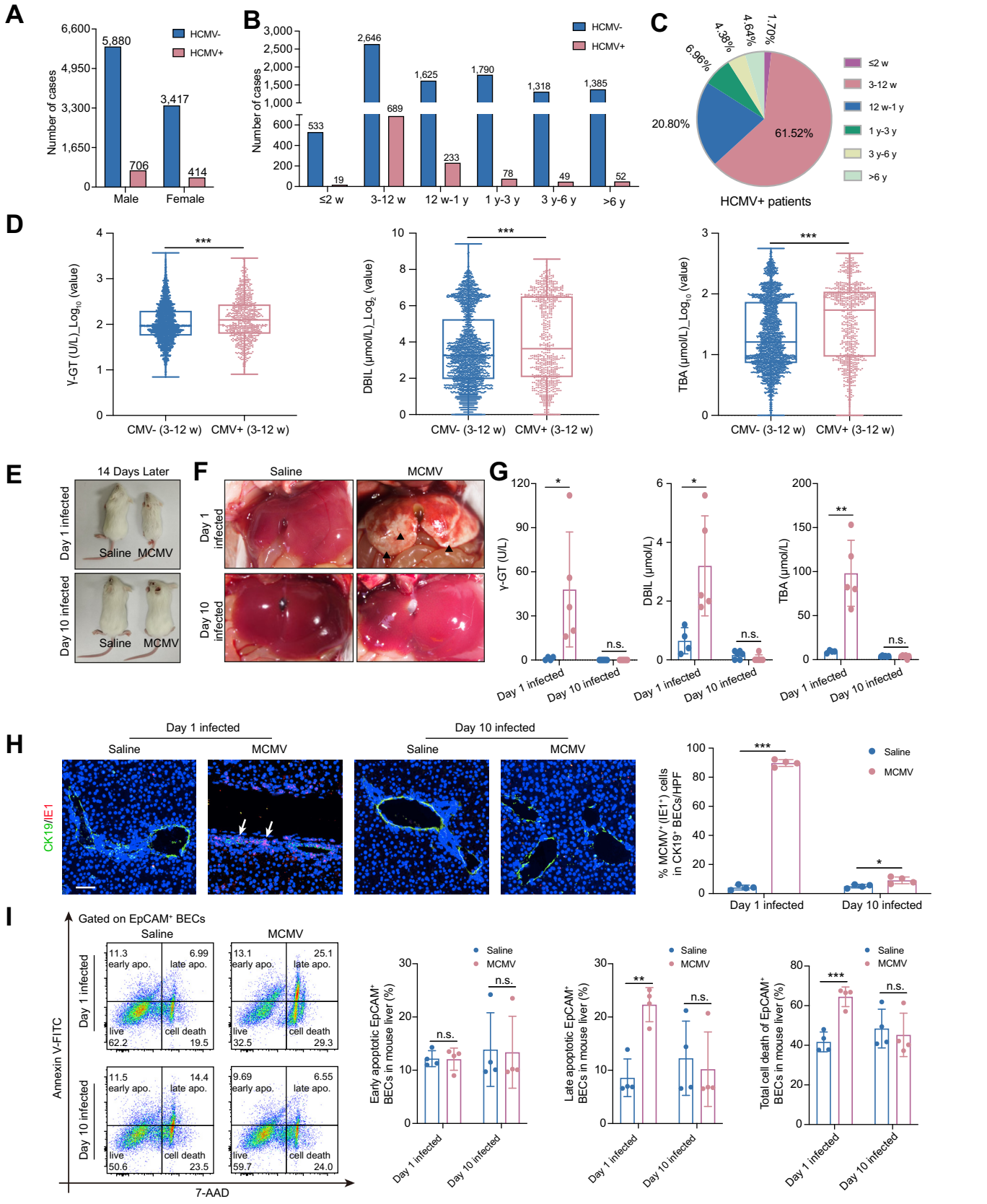

Fig. 1. Perinatal HCMV infection is accompanied by bile duct injury. (A) Number of HCMV+ and HCMV− patients in males and females. (B) Number of HCMV+ and HCMV− patients in different age group. (C) Percentage of HCMV+ patients in each age group. (D) Levels of the bile duct damage-related molecules in the blood of patients with perinatal HCMV infection. Levels of significance: γ-GT: ***p <0.0001; DBIL: ***p <0.0001; TBA: ***p <0.0001 (Mann–Whitney U test). (E) Representative images of BALB/c mice on Day 14 after MCMV inoculation on Day 1 (saline: n = 20; MCMV: n = 20) or Day 10 (saline: n = 18; MCMV: n = 20) after

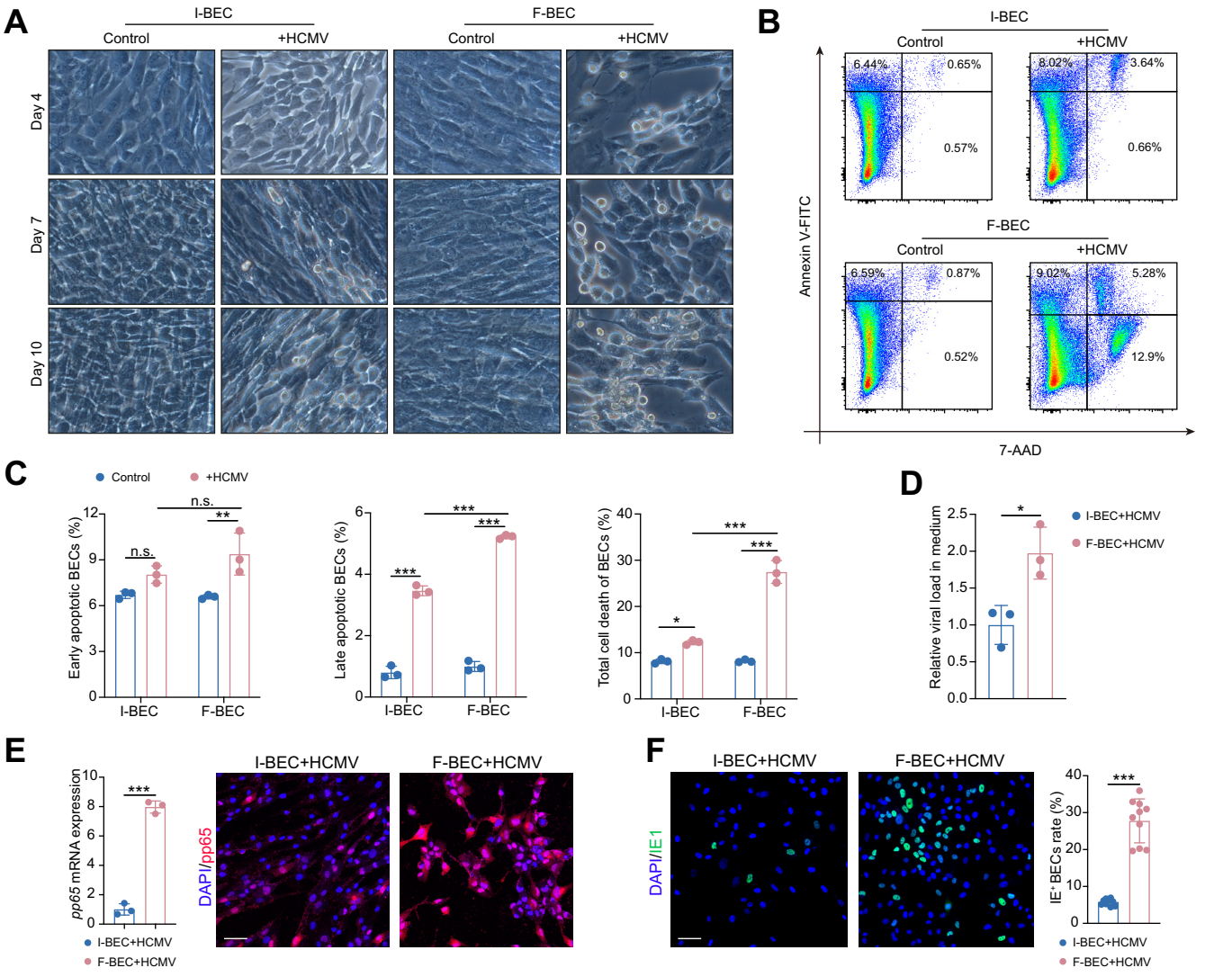

Fig. 2. HCMV infection in F-BECs causes cell death. (A) Representative images of I-BECs and F-BECs cocultured with HCMV at Days 4, 7, and 10. n = 3. (B and C) The total cell death (Annexin-V$^+$, 7-AAD$^+$, and double$^+$) of I-BEC and F-BEC on Day 4 was detected by flow cytometry. n = 3. Levels of significance: early apoptotic, I-BEC: n.s. = 0.2170, F-BEC: $^{**}p$ = 0.0082, I-BEC + HCMV *vs.* F-BEC + HCMV: n.s. = 0.2093; late apoptotic, I-BEC: $^{***}p$ <0.0001, F-BEC: $^{***}p$ <0.0001, I-BEC + HCMV *vs.* F-BEC + HCMV: $^{***}p$ <0.0001; total cell death, I-BEC: $^{*}p$ = 0.0193, F-BEC: $^{***}p$ <0.0001, I-BEC + HCMV *vs.* F-BEC + HCMV: $^{***}p$ <0.0001 (one-way ANOVA). (D) Relative viral load detected by qPCR in the cell culture supernatants of I-BECs and F-BECs cocultured with HCMV on Day 3. n = 3. (E and F) HCMV pp65 mRNA (n = 3) and pp65 protein levels, and IE1 protein level (n = 10) in I-BECs and F-BECs cocultured with HCMV on Day 3 detected by qPCR and immunofluorescence staining. Levels of significance: $^{*}p$ =0.0186 (D); $^{***}p$ <0.0001 (E); $^{***}p$ <0.0001 (F) (two-tailed Student's *t* test). Scale bar: 25 μm. BEC, biliary epithelial cell; F-BEC, fetal biliary epithelial cell; HCMV, human cytomegalovirus; I-BEC, infant biliary epithelial cell; qPCR, quantitative PCR.

cytometry analysis showed that the protein expression of CD55 on EpCAM$^+$ BECs in the livers of mice infected with MCMV was significantly higher than that in the livers of mice inoculated with saline (Figs. S3A and S4F), suggesting the potential role of CD55 in CMV infection in F-BECs. After the administration of siRNA targeting CD55 in F-BECs, reductions in CD55 mRNA and CD55 protein levels were observed (Fig. S4B–D). qPCR and immunofluorescence results showed that the mRNA and protein

birth. (F) Representative images of the liver surface in each group on Day 14. (G) Levels of bile duct damage-related molecules in each group on Day 14. Day 1 infected (saline: n = 4; MCMV: n = 5); Day 10 infected (saline: n = 6; MCMV: n = 6). Levels of significance: γ-GT: $^{*}p$ = 0.0159, n.s. >0.9999; DBIL: $^{*}p$ = 0.0236, n.s. = 0.1504; TBA: $^{**}p$ = 0.0060, n.s. = 0.6015 (two-tailed Student's *t* test). (H) Representative images and quantification of CK19 protein and MCMV IE1 gene double staining of the livers of mice in each group on Day 14. n = 4. Levels of significance: $^{***}p$ <0.0001; $^{*}p$ = 0.0216 (two-tailed Student's *t* test). Scale bar: 50 μm. (I) The total cell death (Annexin-V$^+$, 7-AAD$^+$, and double$^+$) of EpCAM$^+$ BECs in the livers of mice in each group on Day 14 detected by flow cytometry. n = 4. Levels of significance: early apoptotic, Day 1: n.s. = 0.9388, Day 10: n.s. = 0.9190; late apoptotic, Day 1: $^{**}p$ = 0.0012, Day 10: n.s. = 0.6926; total cell death, Day 1: $^{***}p$ = 0.0006, Day 10: n.s. = 0.6792 (two-tailed Student's *t* test). 7-AAD, 7-Aminoactinomycin D; BEC, biliary epithelial cell; CK19, cytokeratin 19; DBIL, direct bilirubin; EpCAM, epithelial cell adhesion molecule; FITC, fluorescein isothiocyanate; γ-GT, γ-glutamyl transpeptidase; HCMV, human cytomegalovirus; HPF, high power field; MCMV, murine cytomegalovirus; TBA, total bile acid.

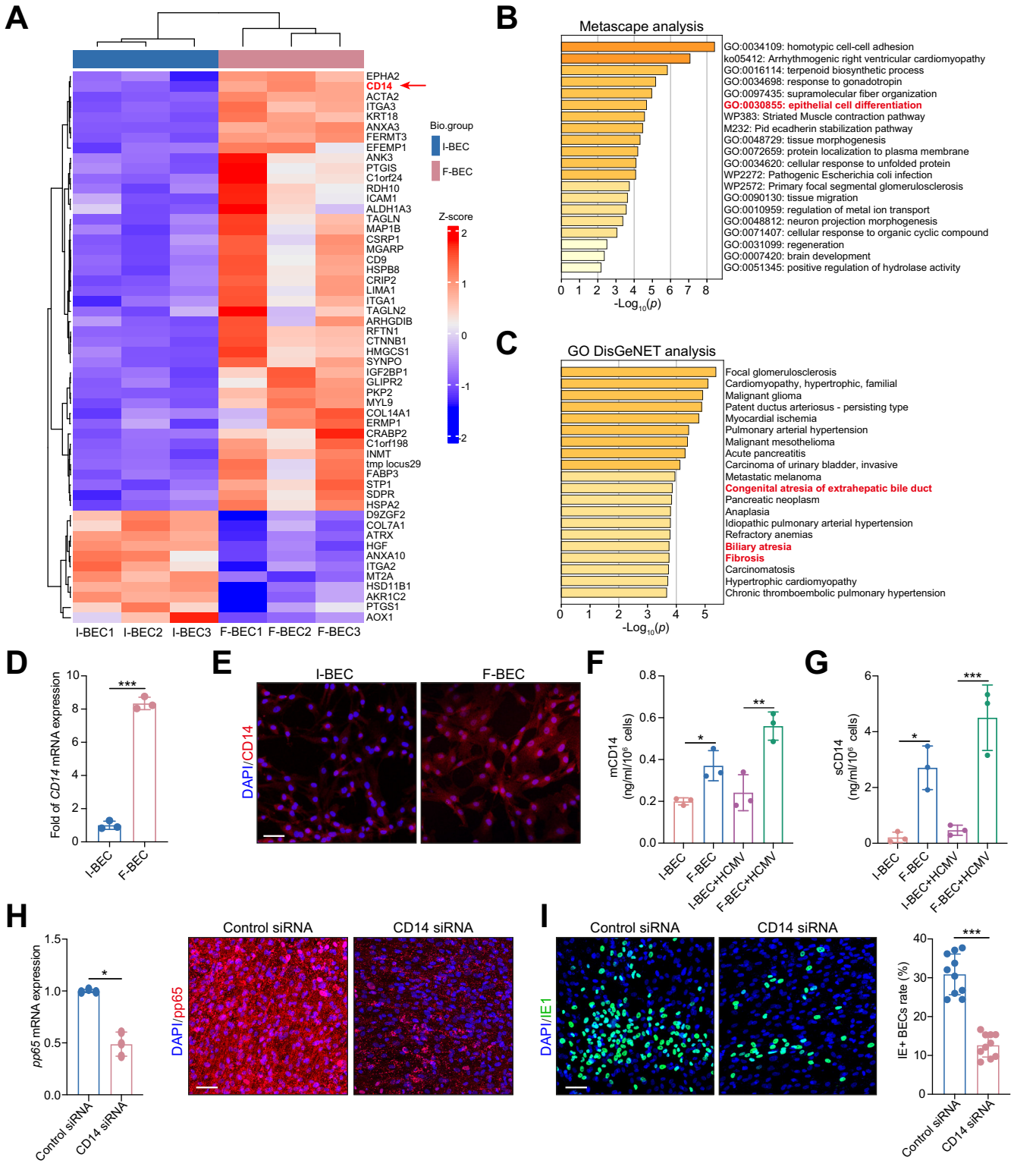

Fig. 3. CD14 produced by F-BECs promotes HCMV infection. (A) Heatmap showing the significantly differentially expressed proteins in F-BECs and I-BECs on Day 3. n = 3. (B and C) The proteins with upregulated expression in F-BECs compared with I-BECs were analyzed using Metascape and GO DisGeNET, respectively, and the proteins involved in the biological functions and related diseases are shown. (D and E) CD14 mRNA and protein expression in F-BECs and I-BECs on Day 3 detected by qPCR and immunofluorescence staining. n = 3. Level of significance: ***p <0.0001 (two-tailed Student's t test). Scale bar: 25 μm. (F and G) mCD14 and sCD14 protein levels in F-BECs and I-BECs with or without HCMV infection on Day 3 detected by ELISA. n = 3. Levels of significance: *p = 0.0163, **p = 0.0016 (F); *p = 0.0119, ***p = 0.0006 (G) (one-way ANOVA). (H and I) HCMV pp65 mRNA (n = 3) and pp65 protein levels, and IE1 protein level (n = 10) in F-BECs treated with control siRNA or CD14 siRNA cocultured with HCMV on Day 3 detected by qPCR and immunofluorescence staining. Levels of significance: *p = 0.0157 (H); ***p <0.0001 (I) (two-tailed Student's t test). Scale bar: 25 μm. BEC, biliary epithelial cell; F-BEC, fetal biliary epithelial cell; GO, gene ontology; HCMV, human cytomegalovirus; I-BEC, infant biliary epithelial cell; mCD14, membrane CD14; qPCR, quantitative PCR; sCD14, soluble CD14.

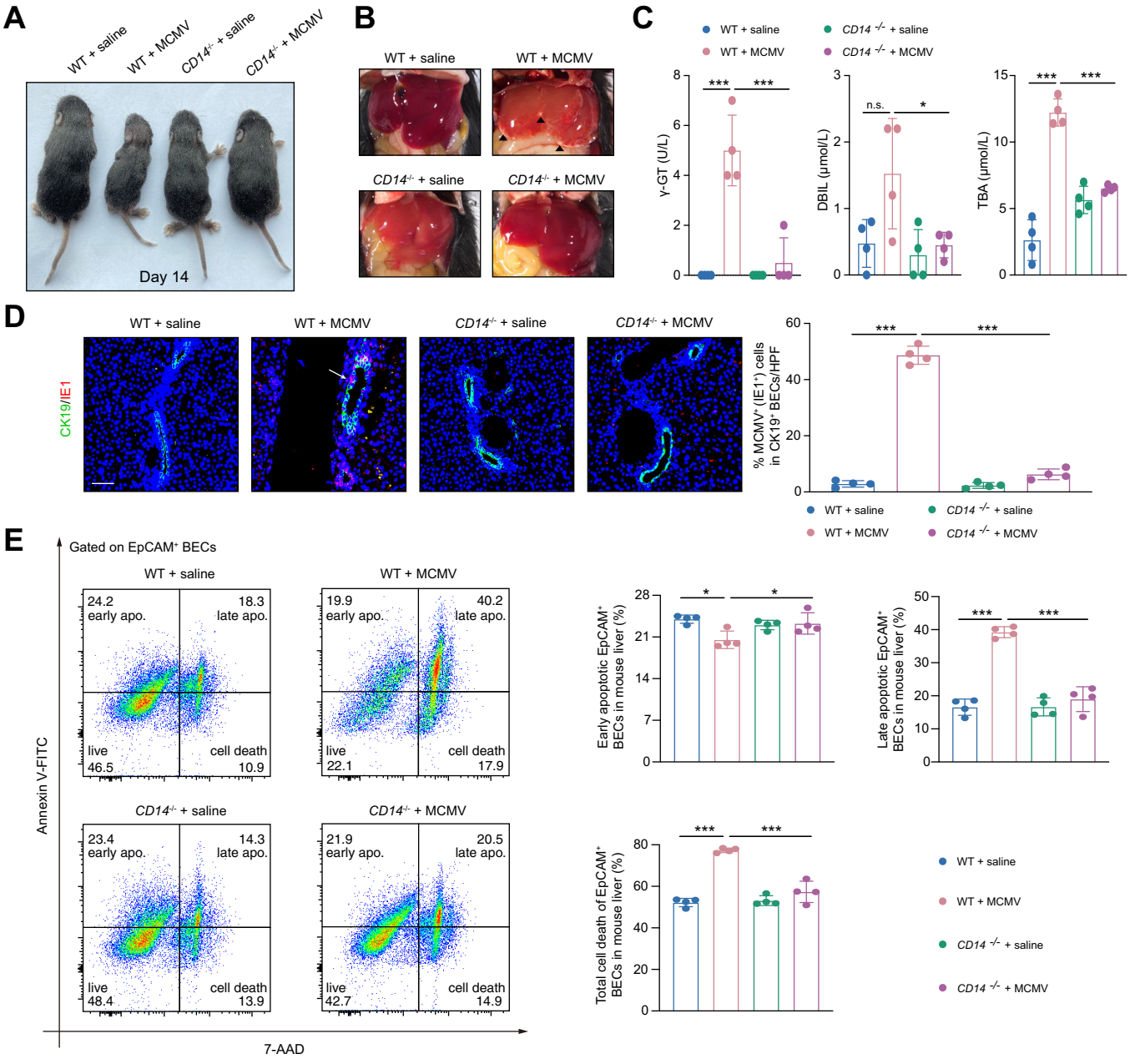

Fig. 4. MCMV infection causes bile duct damage in mice via CD14. (A) Representative images of the mice with a C57BL/6 background in the WT + saline (n = 20), WT + MCMV (n = 15), *CD14*$^{-/-}$ + saline (n = 17), and *CD14*$^{-/-}$ + MCMV (n = 22) groups on Day 14 after inoculation with MCMV on Day 1 after birth. (B) Representative images of the liver surface in each group on Day 14. (C) The levels of bile duct damage-related molecules in each group on Day 14. n = 4. Levels of significance: γ-GT: WT + saline *vs.* WT + MCMV: ***p <0.0001, WT + MCMV *vs.* *CD14*$^{-/-}$ + MCMV: ***p <0.0001; DBIL: WT + saline *vs.* WT + MCMV: n.s. = 0.0501, WT + MCMV *vs.* *CD14*$^{-/-}$ + MCMV: *p = 0.0444; TBA: WT + saline *vs.* WT + MCMV: ***p <0.0001, WT + MCMV *vs.* *CD14*$^{-/-}$ + MCMV: ***p <0.0001 (one-way ANOVA). (D) Representative images and quantification of CK19 protein and MCMV IE1 gene double staining of the livers of mice in each group on Day 14. n = 4. Levels of significance: WT + saline *vs.* WT + MCMV: ***p = 0.0005; WT + MCMV *vs.* *CD14*$^{-/-}$ + MCMV: ***p = 0.0010 (one-way ANOVA). Scale bar: 50 μm. (E) The total cell death (Annexin-V^{+}, 7-AAD^{+}, and double^{+}) of EpCAM^{+} BECs in the livers of mice in each group on Day 14 detected by flow cytometry. n = 4. Levels of significance: early apoptotic, WT + saline *vs.* WT + MCMV: *p = 0.0104, WT + MCMV *vs.* *CD14*$^{-/-}$ + MCMV: *p = 0.0427; late apoptotic, WT + saline *vs.* WT + MCMV: ***p <0.0001, WT + MCMV *vs.* *CD14*$^{-/-}$ + MCMV: ***p <0.0001; total cell death, WT + saline *vs.* WT + MCMV: ***p <0.0001, WT + MCMV *vs.* *CD14*$^{-/-}$ + MCMV: ***p <0.0001 (one-way ANOVA). BEC, biliary epithelial cell; CK19, cytokeratin 19; DBIL, direct bilirubin; EpCAM, epithelial cell adhesion molecule; γ-GT, γ-glutamyl transpeptidase; MCMV, murine cytomegalovirus; TBA, total bile acid; WT, wild-type.

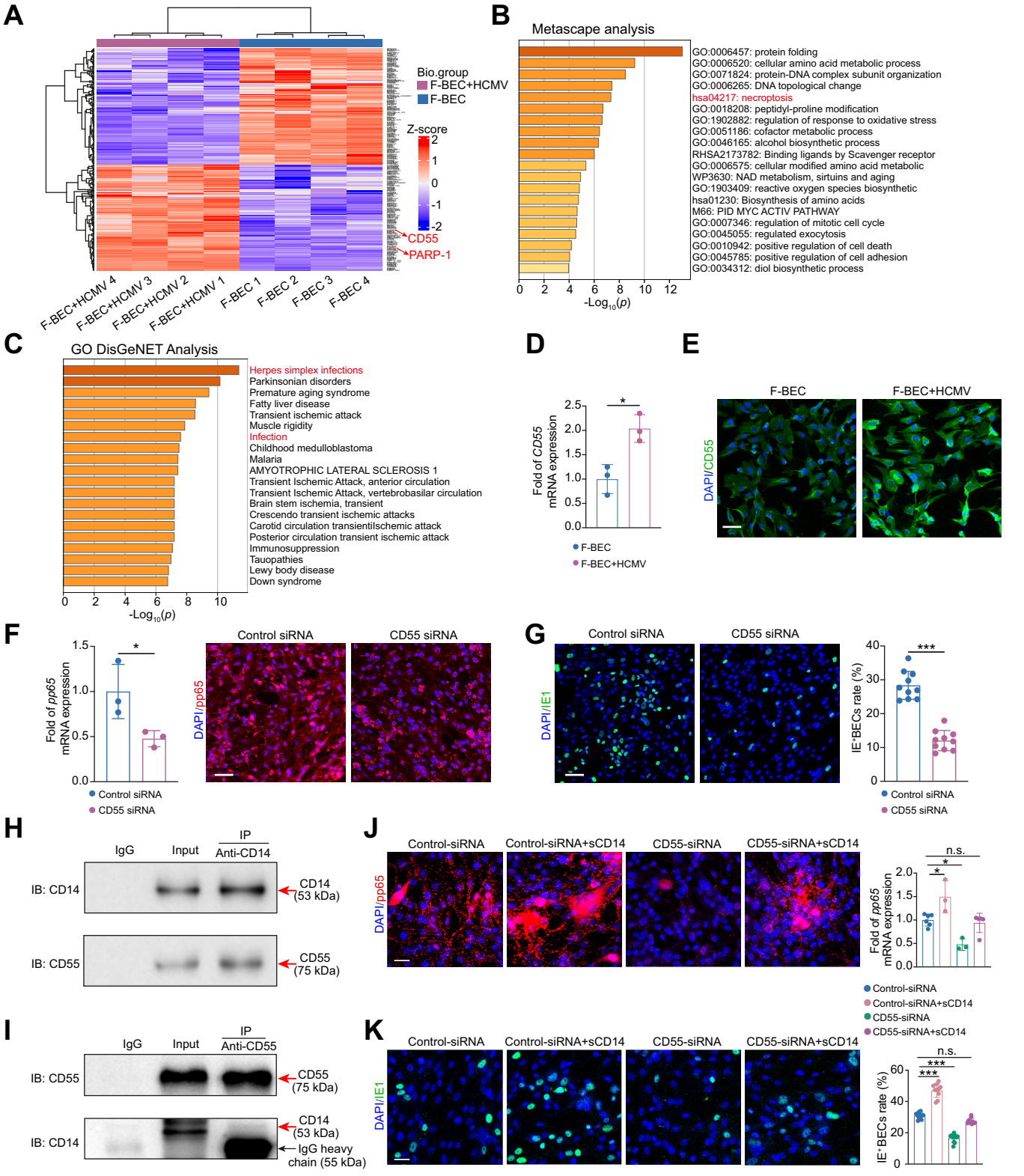

Fig. 5. CD14 promotes HCMV entry into cells partially via CD55 receptor. (A) Heatmap showing the significantly differentially expressed proteins in F-BECs and F-BECs + HCMV on Day 4. n = 4. (B and C) The proteins with upregulated expression in F-BECs + HCMV compared with F-BECs were analyzed using Metascape and GO DisGeNET, respectively, and the proteins involved in biological functions and related diseases are shown. (D and E) CD55 mRNA and protein expression in F-BECs and F-BECs + HCMV on Day 3 detected by qPCR and immunofluorescence staining. n = 3. Levels of significance: $^{*}p = 0.0120$ (two-tailed Student's *t* test). Scale bar: 25 μm. (F and G) HCMV pp65 mRNA and pp65 protein levels (n = 3), and IE1 protein level (n = 10) in F-BECs treated with control siRNA or CD55 siRNA cocultured with HCMV on Day 3 detected by qPCR and immunofluorescence staining. Levels of significance: $^{*}p = 0.0446$ (F); $^{***}p < 0.0001$ (G) (two-tailed Student's *t* test). Scale bar: 25 μm. (H and I) The interaction of CD14 and CD55 in F-BECs cocultured with HCMV on Day 3 detected by coimmunoprecipitation. n = 3. (J and K)

expression of HCMV pp65 and the IE1 protein level in the F-BECs were significantly decreased in the CD55 siRNA group compared with the control group (Fig. 5F and G). These results suggested that HCMV infection can increase CD55 expression in F-BECs and further enhance replication in cells.

To further verify the role of CD14 and CD55 in HCMV infection in F-BECs, protein lysates of F-BECs infected with HCMV were used for immunoprecipitation combined with mass spectrometry analysis. The HCMV structural proteins UL86, UL13, and US22, and the DNA polymerase peptide segment, were detected in the immunoprecipitation protein products of anti-CD14 (Fig. S5A–C), and the HCMV structural protein UL37 was detected in the immunoprecipitation protein products of anti-CD55 (Fig. S5D–F), which indicated that HCMV directly interacts with CD14 and CD55 in the infection process in F-BECs. To verify the relationship between CD14 and CD55 during HCMV infection of F-BECs, we used coimmunoprecipitation to assess the interaction between CD14 and CD55 in F-BECs after HCMV infection. The results showed that CD55 was detected in the immunoprecipitated products of anti-CD14 (Fig. 5H), and CD14 was detected in the immunoprecipitated products of anti-CD55 (Fig. 5I). These results suggest that CD14 binds to CD55 as a complex and is involved in HCMV infection of F-BECs. To further investigate the role of sCD14 and CD55 in HCMV infection of F-BECs, we added recombinant sCD14 to HCMV-infected F-BECs. The results showed that the HCMV pp65 mRNA and protein levels and the number of HCMV IE1-positive F-BECs were significantly increased compared with those of the control group (Fig. 5J and K). Administration of CD55 siRNA reduced the expression of CD55 in F-BECs, and the expression of HCMV pp65 and IE1 was restored to the level of the control siRNA group (Fig. 5J and K). These data suggested that CD55 and CD14 interact to promote HCMV infection in F-BECs.

CD14-neutralizing antibody can alleviate damage to mouse BECs after MCMV infection

To explore the treatment of hepatic bile duct damage in mice infected with MCMV, we injected MCMV i.p. into BALB/c mice on the first day after birth. The CD14-neutralizing antibody biG 53 was given on the second day for 14 consecutive days. The results showed that the antibody alone had no obvious effect on mouse development compared with that of the control (saline) group. However, in the virus infection group, the body weight of the mice treated with the CD14-neutralizing antibody was significantly increased at the end of the experiments (Fig. 6A and Fig. S6A). The survival rate was also increased (Fig. S6B), and liver necrotic spots were not observed (Fig. 6B). The bile duct and hepatocyte injury-related indicators (Fig. 6C and Fig. S6C), the infiltration of immune cells in the portal area, and the number of disordered intrahepatic bile ducts (Fig. S6D–E) were significantly decreased. MCMV immediate early protein IE1 gene expression in BECs was significantly decreased (Fig. 6D), and flow cytometry analysis showed significantly decreased total cell death level of EpCAM$^+$ BECs in the liver (Fig. 6E). These results suggested that treatment with a CD14-neutralizing antibody can improve the damage to BECs in mice infected with MCMV.

The PARP-1 inhibitor PJ34 can alleviate damage to BECs after CMV infection

To further investigate the form and mechanism of cell death of F-BECs after HCMV infection, electron microscopy analysis showed cell membrane disintegration and nuclear reduction in F-BECs after HCMV infection, indicating obvious cell death of F-BECs (Fig. 7A). Based on the significant enrichment of the necroptosis pathway and upregulation of the key cell death molecule PARP-1 in F-BECs observed after HCMV infection (Fig. 5A and B), further examination of PARP-1-mediated cell death signaling pathway molecules showed that PARP-1, cleaved PARP-1, poly ADP-ribose (PAR), and apoptosis-inducing factor (AIF) protein expression increased significantly in F-BECs after HCMV infection (Fig. 7B). MTT and flow cytometry examinations showed that the addition of the PARP-1 inhibitor PJ34 to the medium of F-BECs cocultured with HCMV significantly increased cell activity and hindered F-BEC death (Fig. 7C and D).

To explore the effect of PARP-1 inhibitor on hepatic bile duct damage in mice infected with MCMV, we i.p. injected MCMV into BALB/c mice on the first day after birth. Immunofluorescence staining showed that PARP-1, cleaved PARP-1, PAR, and AIF protein expression increased significantly in CK19$^+$ BECs in the livers of mice after MCMV infection (Fig. S7A). The PARP-1 inhibitor PJ34 was given on the second day for 14 consecutive days, and the results showed that the body weight and survival rate of the mice treated with the PARP-1 inhibitor were significantly increased at the end of the experiments (Fig. S7D). In addition, liver necrotic spots were not observed (Fig. S7B). Significant decreases in the infiltration of immune cells in the portal area, the number of disordered intrahepatic bile ducts (Fig. S7C), and the levels of bile duct and hepatocyte injury-related indicators were observed (Fig. S7E). These results suggested that treatment with the PARP-1 inhibitor PJ34 can improve the damage to BECs in mice infected with MCMV.

Discussion

In this study, we explored the effect of perinatal HCMV infection on BECs and its molecular mechanism. The results showed that F-BECs expressed higher levels of CD14 than I-BECs. This molecule cooperated with cell surface CD55 receptor expression and promoted HCMV infection, and PARP-1-mediated cell death was detected in HCMV-infected F-BECs. Furthermore, the use of a CD14-neutralizing antibody and the PARP-1 inhibitor PJ34

HCMV pp65 mRNA (control-siRNA: n = 6, control-siRNA + sCD14: n = 3, CD55-siRNA: n = 3, CD55-siRNA + sCD14: n = 5) and pp65 protein levels, and IE1 protein level (n = 10) in F-BECs treated with sCD14 and/or in the presence of CD55 siRNA cocultured with HCMV on Day 3 detected by qPCR and immunofluorescence staining. Levels of significance: control-siRNA *vs.* control-siRNA + sCD14: $^*p$ = 0.0184 (J), $^{***}p$ <0.0001 (K); control-siRNA *vs.* CD55-siRNA: $^*p$ = 0.0125 (J), $^{***}p$ <0.0001 (K); control-siRNA *vs.* CD55-siRNA + sCD14: n.s. = 0.9545 (J), n.s. = 0.0534 (K) (one-way ANOVA). Scale bar: 25 μm. BEC, biliary epithelial cell; F-BEC, fetal biliary epithelial cell; GO, gene ontology; HCMV, human cytomegalovirus; IB, immunoblotting; IP, immunoprecipitation; PARP-1, poly ADP-ribose polymerase-1; qPCR, quantitative PCR; sCD14, soluble CD14.

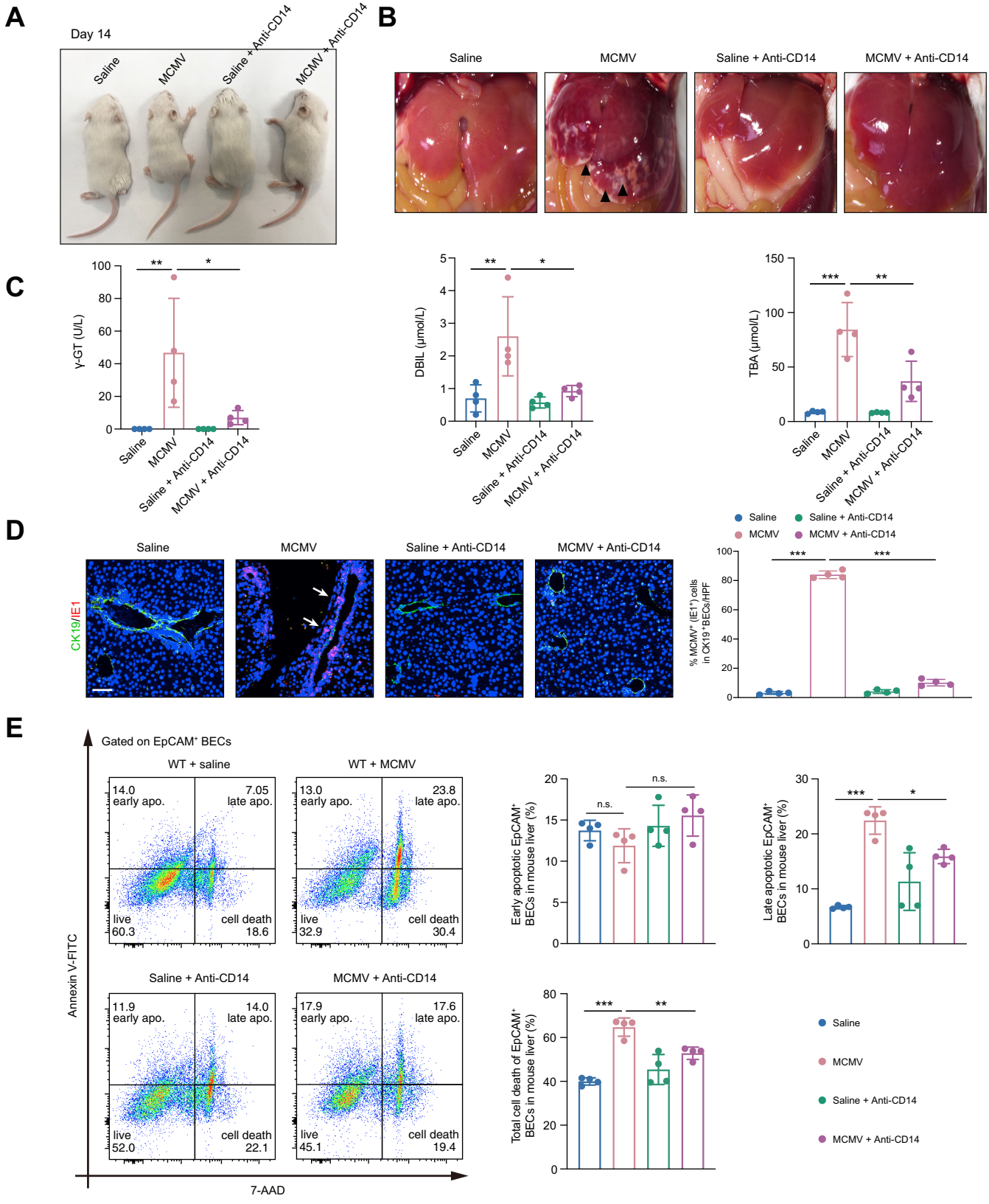

Fig. 6. CD14-neutralizing antibody can alleviate damage to mouse BECs after MCMV infection. (A) Representative images of the mice with a BALB/c background in the saline (n = 18), MCMV (n = 20), saline + anti-CD14 (n = 19), and MCMV + anti-CD14 (n = 20) groups on Day 14 after inoculation with MCMV on Day 1 after birth. (B) Representative images of the liver surface in each group on Day 14. (C) The levels of bile duct damage-related molecules in each group on Day 14. n = 4. Levels of significance: γ-GT: saline *vs.* MCMV: $^{**}p = 0.0093$, MCMV *vs.* MCMV + anti-CD14: $^{*}p = 0.0261$; DBIL: saline *vs.* MCMV: $^{**}p = 0.0067$, MCMV *vs.* MCMV + anti-CD14: $^{*}p = 0.0156$; TBA: saline *vs.* MCMV: $^{***}p < 0.0001$, MCMV *vs.* MCMV + anti-CD14: $^{**}p = 0.0046$; (one-way ANOVA). (D) Representative images

reduced cellular damage in MCMV-infected neonatal mice, suggesting a therapeutic effect.

Multiple HCMV receptors have been identified in recent decades in many different cells.[9,10]

For example, OR14I1 was identified in a retinal pigment epithelial cell line,[11] TLR2 in syncytiotrophoblasts,[12] NRP2 in epithelial/endothelial cells,[9] PDGFRA in U87 glioma cells and human umbilical vein endothelial cells,[13] and EGFR in cytotrophoblasts.[14] However, either the expression of these receptors was not found in the F-BEC/I-BEC database or there was no differences in the HCMV–F-BEC database, suggesting that multiple pathways of virus entry might exist depending on the cell type. Using proteomic analysis with high z scores, we provided new evidence that the interaction between CD14 and CD55 promoted viral infection in F-BECs. Other proteins, such as CTNNB1, KRT18, EFEMP1, and ITGA3, in the same functional group as CD14 showed upregulated expression in F-BECs compared with I-BECs (Fig. S2C), which was potentially related to liver diseases, as shown by GO DisGeNET analysis. However, these proteins showed downregulated expression after HCMV infection (Fig. S4E), suggesting that they might not play an important role in HCMV infection. Interestingly, the expression of ICAM1 was found to be similar to that of CD14, which increased in F-BECs and was further increased after HCMV infection (Fig. S2B and C, and Fig. S4E). ICAM1 expression was shown to be upregulated after HCMV infection in organ transplantation,[15] and ICAM1 can also be expressed in I-BECs and promote cell damage through recruitment of lymphocytes.[16] However, whether ICAM1 interacts with CD14 and CD55 and promotes HCMV invasion should be further investigated.

CD14 is constitutively expressed in many immune cells, such as monocytes and macrophages, as well as in keratinocytes and intestinal epithelial cells.[17] Human BECs express CD14, which is related to the immune response to lipopolysaccharide (LPS).[18] F-BECs highly expressed CD14, and the expression further increased after HCMV infection and sCD14 release. High levels of sCD14 have been shown to be associated with viral infections, such as measles virus,[19] CMV infection,[20] and coinfection with CMV and HIV.[21] A previous study suggested that the sCD14 subtype (sCD14-ST) could be used as a biomarker for sepsis in neonatal infants.[22] As a high level of sCD14 promotes HCMV infection, determining the level of sCD14 together with HCMV in the perinatal period in the presence of a high level of bilirubin will provide valuable information regarding bile duct damage.

CD55 is a complement regulator that is upregulated by and incorporated into HCMV virions for the sake of circumventing complement-mediated neutralization.[23,24] A previous study showed that the presence of sCD14 is important in the binding of LPS to CD55 to form the complex involved in LPS signal transduction.[25] In this study, the level of sCD14 was correlated with perinatal viral infection of BECs in the presence of CD55, suggesting that their interaction promoted virus production in the cells. The details of the interaction, such as the contact region, still need to be further explored. However, CD55 siRNA treatment did not completely block the sCD14-mediated enhancement of HCMV infection (Fig. 5J and K), suggesting that either the reduction by CD55 siRNA is not complete or another cellular receptor cooperates with sCD14 to promote viral infection.

The HCMV structural proteins UL86, UL83, and US22 and DNA polymerase were found in the immunoprecipitation products of anti-CD14 in F-BECs infected with HCMV, and the HCMV structural protein UL37 was found in the immunoprecipitation products of anti-CD55 in F-BECs infected with HCMV, suggesting that their interaction may be one of the factors linking the two molecules. However, the details still need to be further explored. The classical viral proteins that mediate HCMV entry into host cells, such as gB, gM, gO, or pentamers (gH, gL, UL128, UL130, and UL131),[26] were not detected in the immunoprecipitation products of CD14 or CD55 from lysed HCMV-infected F-BECs, suggesting that these molecules might not directly interact with CD14 and CD55. Additional detection techniques and investigations are needed to clarify whether these proteins were used during the process of perinatal HCMV infection in BECs.

In this study, coculture with HCMV resulted in cell death in F-BECs (Fig. 2B and C), and proteomic analysis showed that the necroptosis signaling pathway was significantly enriched (Fig. 5B). Further analysis of the necroptosis signaling pathway found that the expression of three proteins was downregulated and that of nine proteins was upregulated (Fig. S8). Among them, the upregulation of PARP1 expression promotes necroptosis.[27] It was reported that HCMV-related insoluble substances can trigger an increase in the production of reactive oxygen species in human immune cells, leading to PARP-1 activation, AIF nuclear translocation, and DNA fragmentation-related cell death. The addition of an AIF inhibitor can reduce cell death.[28] In this study, PARP-1, cleaved PARP-1, PAR, and AIF protein expression significantly increased in F-BECs after HCMV infection and BECs of mice with MCMV infection. Moreover, the addition of the PARP-1 inhibitor PJ34 significantly reduced the cell death of BECs induced by CMV *in vitro* and *in vivo*. This suggests that PARP-1-mediated cell death was one of the important mechanisms in perinatal HCMV-infected BECs and the therapeutic effect of the PARP-1 inhibitor in bile duct injury.

In conclusion, our results showed that BECs in the perinatal period were more susceptible to HCMV infection owing to the high expression of CD14 and upregulation of CD55 expression after

and statistical analysis of CK19 protein and MCMV IE1 gene double immunofluorescence staining of the liver of mice in each group on Day 14. n = 4. Levels of significance: saline vs. MCMV: ***p <0.0001; MCMV *vs*. MCMV + anti-CD14: ***p <0.0001 (one-way ANOVA). Scale bar: 50 μm. (E) The total cell death (Annexin-V$^+$, 7-AAD$^+$, and double$^+$) of EpCAM$^+$ BECs in the livers of mice in each group on Day 14 detected by flow cytometry. n = 4. Levels of significance: early apoptotic, saline *vs*. MCMV: n.s. = 0.6269, MCMV *vs*. MCMV + anti-CD14: n.s. = 0.1243; late apoptotic, saline *vs*. MCMV: ***p <0.0001, MCMV *vs*. MCMV + anti-CD14: *p = 0.0397; total cell death, saline *vs*. MCMV: ***p <0.0001, MCMV *vs*. MCMV + anti-CD14: **p = 0.0097 (one-way ANOVA). BEC, biliary epithelial cell; CK19, cytokeratin 19; DBIL, direct bilirubin; EpCAM, epithelial cell adhesion molecule; γ-GT, γ-glutamyl transpeptidase; MCMV, murine cytomegalovirus; TBA, total bile acid; WT, wild-type.

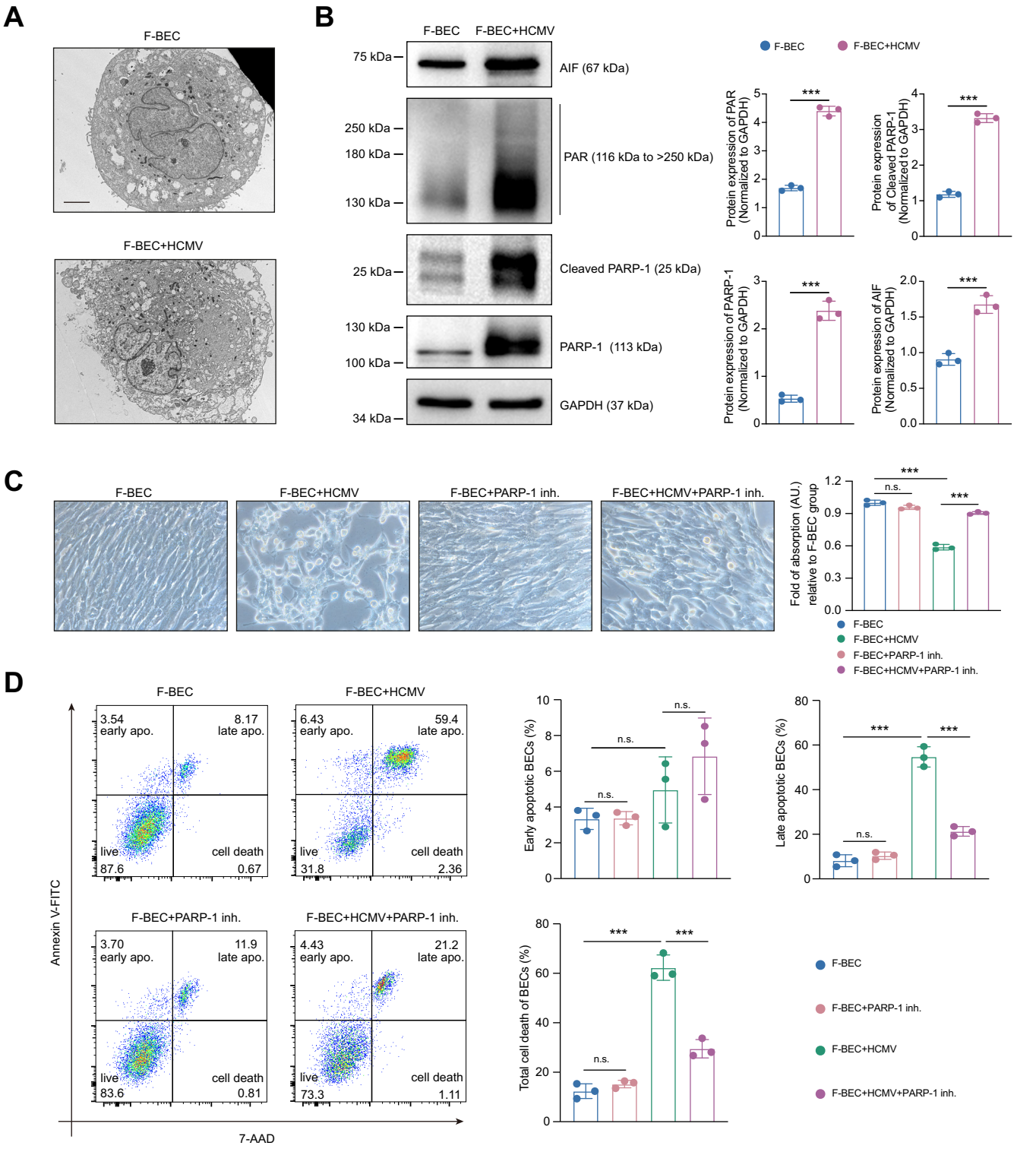

Fig. 7. The PARP-1 inhibitor can improve damage to F-BECs after HCMV infection. (A) Representative electron microscopy images of F-BEC cocultured with HCMV on Day 3. n = 3. Scale bar: 4 μm. (B) The protein expression of PARP-1, cleaved PARP-1, PAR, and AIF in F-BECs cocultured with HCMV on Day 3 detected by Western blot. n = 3. Levels of significance: ***p = 0.0001 (PARP-1), ***p <0.0001 (cleaved PARP-1), ***p <0.0001 (PAR), ***p = 0.0009 (AIF) (two-tailed Student's t test). (C) Representative images of F-BECs cocultured with HCMV with PARP-1 inh. on Day 3. The proliferation of F-BECs was detected by the MTT assay. n = 3. Levels of significance: n.s. = 0.1339, F-BEC *vs.* F-BEC + HCMV: ***p <0.0001, F-BEC + HCMV *vs.* F-BEC + HCMV + PARP-1 inh.: ***p <0.0001 (one-way ANOVA). (D) The total cell death (Annexin-V$^+$, 7-AAD$^+$, and double$^+$) of F-BECs in each group on Day 3 detected by flow cytometry. n = 3. Levels of significance: early apoptotic, F-BEC *vs.* F-BEC + PARP-1 inh.: n.s. >0.9999, F-BEC *vs.* F-BEC + HCMV: n.s. = 0.5528, F-BEC + HCMV *vs.* F-BEC + HCMV + PARP-1 inh.: n.s. = 0.4400; late apoptotic, F-BEC *vs.* F-BEC + PARP-1 inh.: n.s. = 0.7946, F-BEC *vs.* F-BEC + HCMV: ***p <0.0001, F-BEC + HCMV *vs.* F-BEC + HCMV + PARP-1 inh.: ***p <0.0001; total cell death, F-BEC *vs.* F-BEC + PARP-1 inh.: n.s. = 0.7623, F-BEC *vs.* F-BEC + HCMV: ***p <0.0001, F-BEC + HCMV *vs.* F-BEC + HCMV + PARP-1 inh.: ***p <0.0001 (one-way ANOVA). AIF, apoptosis-inducing factor; BEC, biliary epithelial cell; F-BEC, fetal biliary epithelial cell; HCMV, human cytomegalovirus; inh., inhibitor; PAR, poly ADP-ribose; PARP-1, poly ADP-ribose polymerase-1.

HCMV infection. The two molecules form a complex to promote perinatal HCMV infection of BECs, and PARP-1-mediated cell death was detected in perinatal CMV-infected BECs. Targeting the expression of CD14/sCD14 and/or the expression of CD55 and PARP-1 may be a potentially effective treatment for perinatal bile duct injury caused by HCMV infection.

Abbreviations

AIF, apoptosis-inducing factor; ALP, alkaline phosphatase; ALT, alanine aminotransferase; AST, aspartate aminotransferase; BEC, biliary epithelial cell; CK19, cytokeratin 19; CMV, cytomegalovirus; DBIL, direct bilirubin; EpCAM, epithelial cell adhesion molecule; F-BEC, fetal biliary epithelial cell; γ-GT, γ-glutamyl transpeptidase; GO, gene ontology; HCMV, human cytomegalovirus; I-BEC, infant biliary epithelial cell; IB, immunoblotting; IBIL, indirect bilirubin; IP, immunoprecipitation; LPS, lipopolysaccharide; mCD14, membrane CD14; MCMV, murine cytomegalovirus; PAR, poly ADP-ribose; PARP-1, poly ADP-ribose polymerase-1; qPCR, quantitative PCR; sCD14, soluble CD14; TBA, total bile acid; TBIL, total bilirubin; WT, wild-type.

Financial support

This work was supported by the National Natural Science Foundation of China (82201894), China Postdoctoral Science Foundation (2022M720894), Basic and Applied Basic Research, and the Science and Technology Planning Project of Guangzhou (No. 2023A04J1221) to LS; Macau Science and Technology Development Fund (0086/2022/A) to YC; the Open Research Fund Program of the State Key Laboratory of Virology of China (2015IOV006 and 2018IOV005) to RZ; and the Science and Technology Planning Project of Guangdong Province (No. 2019B020227001) and the Science and Technology Planning Project of Guangzhou (No. 202206080002) to HX.

Conflicts of interest

The authors have declared that no conflict of interest exists.

Please refer to the accompanying ICMJE disclosure forms for further details.

Authors' contributions

Performed the experiments: LS, YC, MF, HW, YT, ZL, HC, HL, SM, YX, JH, ZZ, FL, HS, RZ. Recruited patient, provided clinical information, and performed clinical care: LS, MF, Zhe Wang, JZ, WZ, HX, RZ. Responsible for sample collection: LS, MF, Yi Chen, BZ, RZ. Performed bioinformatic and statistical analysis: LS, YC, RZ, RY. Wrote the manuscript: LS. Provided significant input: ML, YC, HX, RZ. Conceived and supervised the project: LS.

Data availability statement

Further information and request for resources and reagents should be directed to the Lead Contact Professor HX (xia-huimin@foxmail.com) or RZ (zhangruizhong@gwcmc.org). Data and code availability: The raw sequencing data that support the findings of this study were deposited in the OMIX, China National Center for Bioinformation/Beijing Institute of Genomics, Chinese Academy of Sciences. Official website: *https://ngdc.cncb.ac.cn/omix*. Accession No. OMIX002966. Publicly available databases and software are specified in the Supplementary CTAT Table.

Acknowledgements

The authors would like to thank the State Key Laboratory of Virology (Wuhan University, China) for providing the MCMV K181 strain and HCMV Towne strain.

Supplementary data

Supplementary data to this article can be found online at https://doi.org/10.1016/j.jhepr.2024.101018.

References

Author names in bold designate shared co-first authorship

[1] Zuhair M, Smit GSA, Wallis G, et al. Estimation of the worldwide seroprevalence of cytomegalovirus: a systematic review and meta-analysis. Rev Med Virol 2019;29:e2034.

[2] Fang FQ, Fan QS, Yang ZJ, et al. Incidence of cytomegalovirus infection in Shanghai, China. Clin Vaccin Immunol 2009;16:1700–1703.

[3] Liu LW, Qian JH, Zhu TW, et al. [A 5-year retrospective clinical study of perinatal cytomegalovirus infection]. Zhongguo Dang Dai Er Ke Za Zhi 2016;18:99–104.

[4] Wood AM, Hughes BL. Detection and prevention of perinatal infection: cytomegalovirus and Zika virus. Clin Perinatol 2018;45:307–323.

[5] Coclite E, Di Natale C, Nigro G. Congenital and perinatal cytomegalovirus lung infection. J Matern Fetal Neonatal Med 2013;26:1671–1675.

[6] Hasosah MY, Kutbi SY, Al-Amri AW, et al. Perinatal cytomegalovirus hepatitis in Saudi infants: a case series. Saudi J Gastroenterol 2012;18:208–213.

[7] Bezerra JA, Wells RG, Mack CL, et al. Biliary atresia: clinical and research challenges for the twenty-first century. Hepatology 2018;68:1163–1173.

[8] Kosai K, Kage M, Kojiro M. Clinicopathological study of liver involvement in cytomegalovirus infection in infant autopsy cases. J Gastroenterol Hepatol 1991;6:603–608.

[9] Martinez-Martin N, Marcandalli J, Huang CS, et al. An Unbiased screen for human cytomegalovirus identifies neuropilin-2 as a central viral receptor. Cell 2018;174:1158–1171.e1119.

[10] Hein MY, Weissman JS. Functional single-cell genomics of human cytomegalovirus infection. Nat Biotechnol 2022;40:391–401.

[11] E X, Meraner P, Lu P, et al. OR14I1 is a receptor for the human cytomegalovirus pentameric complex and defines viral epithelial cell tropism. Proc Natl Acad Sci U S A 2019;116:7043–7052.

[12] Chan G, Guilbert LJ. Ultraviolet-inactivated human cytomegalovirus induces placental syncytiotrophoblast apoptosis in a Toll-like receptor-2 and tumour necrosis factor-alpha dependent manner. J Pathol 2006;210:111–120.

[13] Soroceanu L, Akhavan A, Cobbs CS. Platelet-derived growth factor-alpha receptor activation is required for human cytomegalovirus infection. Nature 2008;455:391–395.

[14] Maidji E, Genbacev O, Chang HT, et al. Developmental regulation of human cytomegalovirus receptors in cytotrophoblasts correlates with distinct replication sites in the placenta. J Virol 2007;81:4701–4702.

[15] Abele-Ohl S, Leis M, Wollin M, et al. Human cytomegalovirus infection leads to elevated levels of transplant arteriosclerosis in a humanized mouse aortic xenograft model. Am J Transpl 2012;12:1720–1729.

[16] Yokomori H, Oda M, Ogi M, et al. Expression of adhesion molecules on mature cholangiocytes in canal of Hering and bile ductules in wedge biopsy samples of primary biliary cirrhosis. World J Gastroenterol 2005;11:4382–4389.

[17] Bas S, Gauthier BR, Spenato U, et al. CD14 is an acute-phase protein. J Immunol 2004;172:4470–4479.

[18] Harada K, Ohira S, Isse K, et al. Lipopolysaccharide activates nuclear factor-kappaB through toll-like receptors and related molecules in cultured biliary epithelial cells. Lab Invest 2003;83:1657–1667.

[19] Mascia C, Pozzetto I, Kertusha B, et al. Persistent high plasma levels of sCD163 and sCD14 in adult patients with measles virus infection. PLoS One 2018;13:e0198174.

[20] Zipfel A, Schenk M, Grenz A, et al. TNF-α and sCD14 as early markers of CMV susceptibility after liver transplantation. Transpl Proc 2001;33:1794–1795.

[21] Lurain NS, Hanson BA, Hotton AL, et al. The association of human cytomegalovirus with biomarkers of inflammation and immune activation in HIV-1-infected women. AIDS Res Hum Retroviruses 2016;32:134–143.

[22] van Maldeghem I, Nusman CM, Visser DH. Soluble CD14 subtype (sCD14-ST) as biomarker in neonatal early-onset sepsis and late-onset sepsis: a systematic review and meta-analysis. BMC Immunol 2019;20:17.

[23] Spiller OB, Morgan BP, Tufaro F, et al. Altered expression of host-encoded complement regulators on human cytomegalovirus-infected cells. Eur J Immunol 1996;26:1532–1538.

[24] Spear GT, Lurain NS, Parker CJ, et al. Host cell-derived complement control proteins CD55 and CD59 are incorporated into the virions of two unrelated enveloped viruses. Human T cell leukemia/lymphoma virus type I (HTLV-I) and human cytomegalovirus (HCMV). J Immunol 1995;155:4376–4381.

[25] Schletter J, Brade H, Brade L, et al. Binding of lipopolysaccharide (LPS) to an 80-kilodalton membrane protein of human cells is mediated by soluble CD14 and LPS-binding protein. Infect Immun 1995;63:2576–2580.

[26] Griffiths P, Reeves M. Pathogenesis of human cytomegalovirus in the immunocompromised host. Nat Rev Microbiol 2021;19:759–773.
[27] Galluzzi L, Kepp O, Krautwald S, et al. Molecular mechanisms of regulated necrosis. Semin Cel Dev Biol 2014;35:24–32.
[28] **Kim JH**, **Kim J**, Roh J, et al. Reactive oxygen species-induced parthanatos of immunocytes by human cytomegalovirus-associated substance. Microbiol Immunol 2018;62:229–242.